In situ ^{119}Sn Mössbauer Effect Study of Li−$CoSn_2$ Electrochemical System

C. M. Ionica-Bousquet, P. E. Lippens,* L. Aldon, J. Olivier-Fourcade, and J. C. Jumas

Laboratoire des Agrégats Moléculaires et Matériaux Inorganiques (CNRS UMR 5072), Université Montpellier II, CC 015, Place E. Bataillon, 34095 Montpellier cedex 5, France

Received September 8, 2006

Crystalline $CoSn_2$ powders prepared by a ceramic route under an Ar/H_2 controlled atmosphere are examined as a negative electrode for lithium-ion batteries. Ex situ X-ray diffraction measurements show that an electrochemically driven solid-state transformation of $CoSn_2$ occurs during the first reaction period. The complete reaction mechanism of $CoSn_2$ is investigated by in situ ^{119}Sn Mössbauer spectroscopy using a Li-ion plastic cell. The conversion reaction proceeds through a biphasic system, with $CoSn_2$ direct transformation into both a lithium-rich Li_ySn (where $y \approx 3.5$) compound and metallic Co nanoparticles. On charge, the electrochemical process is more complex and it includes the conversion of the Li_ySn compound into a modified $CoSn_2$ nanocompound with a variable composition, i.e., a $Li_yCo_zSn_2$ matrix, which is the active species for the following cycles.

Introduction

In response to the growing demand for portable electronic devices with higher performances, a worldwide effort has been made to find alternative positive and negative active materials for Li-ion batteries. Attempts have been made to replace commonly used carbonaceous negative materials by lithium systems Li_xM (M = Sn, Sb, Si), as they show larger specific capacities.[1] Unfortunately, most Li_xM systems are brittle and can be easily pulverized by the large Li-driven volume variation during the charge and discharge reactions. Both electrode mechanical disintegration and loss of electrical contact between the particles cause poor cyclability.[2] There is a great interest for intermetallic materials (MM′) formed by a lithium reactive component (M) and an inactive one (M′). Their functioning is based on alloy-formation reactions, described as displacement reactions in which M forms a lithium alloy Li_xM. Nanoparticles M′ are also created. The inactive matrix formed by these nanoparticles may buffer the volume expansion of the active phase.

The tin- and transition-metal-based intermetallic systems[3,4] or composites[5] were intensively studied as negative electrode materials in order to use the large reversible lithium-storage capability of tin (maximum uptake of tin is $Li_{4.4}Sn$, corresponding to 990 A h kg^{-1}) as well as to study the inactive matrix effect of transition metals for better cycling performances. The interest in these materials has risen since the commercialization by Sony Company of the newly developed tin-based (Co−Sn−C) component anode[6,7] with improved cyclability.

Our research deals with the MSn_2 stannides with a $CuAl_2$ (C16) type structure, where M is a transition metal (Co, Fe, Mn). The $CuAl_2$ structure has a tetragonal unit cell, space group *I*4/*mcm*, in which Sn atoms occupy the 8*h* sites and M atoms occupy the 4*a* sites. The M atom is surrounded by 8 Sn atoms located at the corners of a square antiprism, with two additional M neighbors along the *c*-axis forming linear chains, whereas the nearest neighbors of each Sn atom are 4 M atoms.[8,9] The electrochemical lithium reaction with these compounds often takes place through multiphase mechanisms, and the X-ray diffraction patterns of the discharged/charged electrodes do not show well-defined peaks. The use of an alternative technique such as in situ Mössbauer spectrometry is suitable for investigating the electrochemical reactions of the anode material at the atomic scale.[10−12]

This paper describes the synthesis of crystalline $CoSn_2$ powders. The electrochemical performance of these powders as electrodes in lithium cells is evaluated and the reaction mechanism with lithium is investigated by ex situ XRD and in situ ^{119}Sn Mössbauer spectroscopy.

Experimental Section

$CoSn_2$ was prepared directly from the elements by solid-state synthesis. Every element had a 99.9% stated purity or better.

* Corresponding author. E-mail: lippens@univ-montp2.fr.

(1) Huggins, R. A. *Handbook of Battery Materials*; Besenhard, J. O., Ed.; Wiley-VCH: Weinheim, Germany, 1999.
(2) Besenhard, J. O.; Yang, J.; Winter, M. *J. Power Sources* **1997**, *68*, 87.
(3) Mao, O.; Turner, R. L.; Courtney, I. A.; Fredericksen, B. D.; Buckett, M. I.; Krause, L. J.; Dahn, J. R. *Electrochem. Solid State Lett.* **1999**, *2* (1), 3−5.
(4) Sharma, S.; Fransson, L.; Sjöstedt, E.; Nordström, L.; Johansson, B.; Edström, K. *J. Electrochem. Soc.***2003**, *150*, *3*, A330.
(5) Beaulieu, L. Y.; Larcher, D.; Dunlap, R. A.; Dahn, J. R. *J. Alloys Compd.* **2000**, *297*, 122.
(6) Sony. U.S. Patent 0053131, 2005.
(7) http://www.sony.net/SonyInfo/News/press/200502/05-006E/.
(8) Havinga, E. E.; Damsma, H.; Hokkeling, P. *J. Less-Common Met.* **1972**, *27*, 169.
(9) Kouvel, J. S.; Hartelius, C. C. *J. Phys. Rev.* **1961**, *123*, 1.
(10) Aldon, L.; Kubiak, P.; Garcia, A.; Lippens, P.-E.; Olivier-Fourcade, J.; Jumas, J.-C. *Hyperfine Interact.* **2004**, *156−157*, 497−503.
(11) Jumas, J.-C.; Robert, F.; Aldon, L.; Skordeva, E. *J. Optoelectron. Adv. Mater.* **2005**, *7* (*1*), 177−184.
(12) Robert, F.; Lippens, P.-E.; Olivier-Fourcade, J.; Jumas, J.-C.; Morcrette, M. *J. Power Sources* **2005**, *146*, 492−495.

10.1021/cm062132i CCC: $33.50
Published on Web 12/19/2006

Appropriate amounts of the constituent elements, i.e., metallic cobalt and tin, were placed in an alumina crucible in a furnace (79300 Thermolyne Tube Furnace) under a controlled Ar/H_2 (5%) atmosphere and resistance-heated at a 480 °C temperature for about 6 h. To obtain a homogeneous sample, we annealed the compound at 350 °C.

After preparation, the compound was crushed in an agate mortar and powder X-ray diffraction (PHILIPS X'Pert MPD equipped with the X'celerator detector) pattern was recorded using Cu Kα radiation in $\theta-2\theta$ continuous mode to determine the structural properties of the sample.

The powdered samples were observed by scanning electron microscopy (SEM) in order to characterize both the sample morphology and the particle size. The particle size distribution was measured with a MALVERN Instruments laser diffraction particle analyzer, in which the suspensions were treated with ultrasound before and during the measurement in order to break larger aggregates in the suspension down to smaller ones. X-ray fluorescence spectroscopy (XRF) was used to measure the elemental composition of the material.

Electrodes containing 80 wt % sample, 10 wt % polytetrafluoroethylene (PTFE) binder, and 10 wt % carbon black (Y50A) were prepared for cycling tests. Standard Swagelok cells Li|1 M $LiPF_6$ (propylenecarbonate (PC):ethylene carbonate (EC):dimethyl carbonate (DMC) = 1:1:3, v/v)|$CoSn_2$ were assembled in an argon-filled glove box and tested using a Mac Pile II system at a rate of C/8 for both charge and discharge, between 0.02 and 1.4 V versus Li^+/Li.

To identify the electrode reaction mechanism, we carried out XRD for $CoSn_2$-lithiated electrodes discharged and charged at several depths of the electrochemical reaction, using a current density of 0.12 mA cm^{-2}. The cells were opened inside the glove box and the electrode materials containing the active material were placed on a specific sample holder transparent for X-rays.

For the room temperature in situ ^{119}Sn Mössbauer measurements in transmission mode, the positive electrode was made according to the Bellcore technology[13,14] by mixing 56 wt % $CoSn_2$ active material, 6 wt % conducting SP carbon black, 15 wt % 88/12 poly vinylidene fluoride/hexafluoropropylene (PVDF/HFP) copolymer, and 23 wt % dibutylphtalate (DBP) acting as a plasticizer. A rectangle plastic electrode of 2/2.5 cm containing 55 mg of $CoSn_2$ was punched out of the plastic laminate. Before this electrode was used in the electrochemical cell, the DBP was extracted by soaking in anhydrous ether. The cells were assembled in an argon-filled glove box and sealed in airtight aluminized plastic bags. The electrode loading was of 11 mg cm^{-2}.

The electrochemical cell, directly monitored by the Mac Pile (Biologic) system operating in galvanostatic mode, has been introduced in a computer-driven EG&G constant acceleration Mössbauer spectrometer. Here, the discharging (reaction of positive $CoSn_2$ electrode with lithium) and charging (lithium-removal process) rate was lowered from C/8 to C/20 (current density of 0.05 mA cm^{-2}) to give the reactions time to reach completion. The Mössbauer data were recorded continuously in consecutive 2 h scans. Each spectrum corresponds to 0.1 discharged or charged lithium electrode compositions. The source was ^{119}Sn in a $CaSnO_3$ matrix. The velocity scale was calibrated using the magnetic sextuplet of a high-purity iron foil absorber as a standard and using ^{57}Co(Rh) as the source. The tin Mössbauer spectra were fitted with a least-squares program, GM5SIT,[15−16] using the Lorentzian profiles. The program gives the isomer shift δ (with respect to $BaSnO_3$ spectrum at room temperature) and the quadrupole splitting Δ. The fitting quality was controlled by the classical χ^2 test and the "misfit" test.

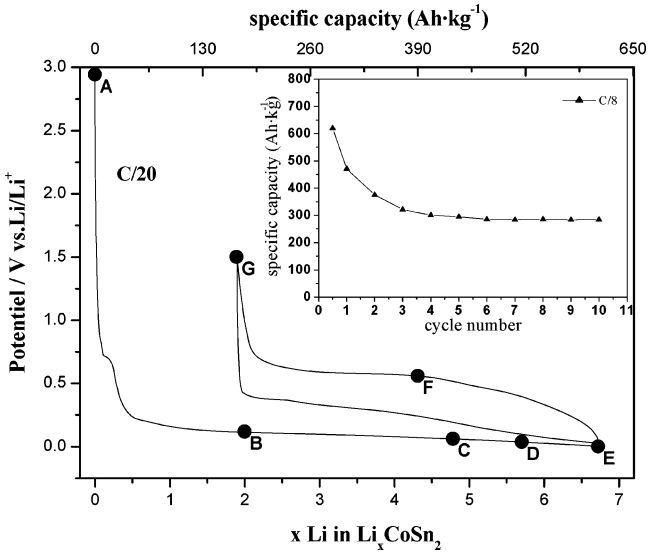

Figure 1. Charge and discharge curve of $CoSn_2$ electrode in a Swagelok cell at a rate of C/20. For the A−G compositions, X-ray measurements have been performed. The inset shows cycle behavior of the compound at rate of C/8.

Results and Discussions

Electrochemical Measurements. Figure 1 illustrates the charge−discharge curve of the Li/$CoSn_2$ Swagelok cell at a rate of C/20. The discharge potential for the $CoSn_2$ electrode rapidly drops to 0.8 V vs Li. This process leads to the formation of a SEI (solid electrolyte interface) passivating film as a result of the reduction reactions of Li with electrolyte taking place on the carbon particles.[17] The electrochemical reduction process occurs at very low voltage, i.e., between 0.14 and 0 V versus Li^+/Li. Those reaction potentials are lower than those of the metallic β-Sn electrode characterized by a few alloying/dealloying reactions, which are represented by several voltage plateaus corresponding to the formation of Li_xSn intermediate stable phases.

The end of the discharge process at 0 V corresponds to the reaction of approximately 7 Li per $CoSn_2$ formula unit. The first discharge capacity was ca. 620 A h kg^{-1}, and the reversible specific capacity in the first cycle was 450 A h kg^{-1}, which suggests that by employing a new electrode material such as $CoSn_2$, which has a high energy density, we can achieve a long-term use of the battery.[18] It is noteworthy that if we consider the $CoSn_2$ density (ρ = 8.91 g cm^{-3}), then the volumetric capacity is 3890 A h m^{-3}, which is much larger than that of the graphite electrode (800 A h m^{-3}). Electrode capacity fading may be due to the high volume expansion, as presented in Figure 1.

X-ray Diffraction. The interpretation of the X-ray diffraction pattern yielded two kinds of results. On the one hand, the sample purity has been checked. On the other hand, the

(13) Tarascon, J.-M.; Gozdz, A. S.; Schmutz, C.; Shokoohi, F.; Warren, P. C. *Solid State Ionics* **1996**, *86−88*, 49−54.
(14) Guyomard, D.; Tarascon, J.-M. U.S. Patent 5192629, 1993.
(15) Ruebenbauer, K.; Birchall, T. *Hyperfine Interact.* **1979**, *7*, 175.
(16) Aldon L.; Jumas, J.-C. *Mössbauer Eff. Ref. Data J.* **2005**, *28* (10) p.2.
(17) Cheng, X.-Q.; Shi, P.-F. *J. Alloys Compd.* **2005**, *391*, 241−244.
(18) Hiroyuki; H.; Takuya; I.; Yasufumi; N.; Yasuhiko, B.; Shinji; K.; Yoshiaki, N. U.S. Patent 6882130, 2005.

Table 1. Compositions of $CoSn_2$ Electrodes Prepared by Discharge at a Rate of C/20 and Refined Cell Parameters

sample	x in Li_xCoSn_2	a (Å)	c (Å)	V (Å^3)
A	0	6.364(2)	5.456(1)	220.92
B	2	6.383(7)	5.463 (2)	222.58
C	4.8	6.371(3)	5.454(6)	221.47

a and c parameters of the tetragonal $CuAl_2$-type unit cell were determined. They were calculated with a least-squares computer program. The parameter values obtained are listed in Table 1 and closely agree with those previously reported for $CoSn_2$, which has an ordered tetragonal $CuAl_2$ structure (a = 6.363 Å and c = 5.456 Å).[19] Fluorescence X-ray measurements made it possible to estimate the real composition of 67.6 at % Sn. SEM and laser diffraction images of the powdered samples were used to estimate the particle size, which ranged from 2 to 6 μm.

To study the reaction mechanism and to observe the structural modifications induced by the oxido-reduction process, we performed ex situ X-ray diffraction measurements on the $CoSn_2$ electrodes. Figure 2 shows the progressive changes of the X-ray profile during discharge (samples A−E) and charge (samples F and G). The major peaks from the raw material (sample A) are indicated on the figure. The comparison between the XRD diagrams of the A and B (2Li) samples reveals some similarity, i.e., the peak intensities were not significantly modified and only a slight modification of the HWHM was observed. This clearly shows that the reaction of $CoSn_2$ with 2 Li ions does not lead to a significant structural modification or to the amorphization of the starting electrode material. However, the refinement of the unit-cell parameters performed for the B sample reveals a slight increase in the cell parameters. If we consider that this slight change in lattice parameters is very important for the reaction mechanism, then a possible solid-solution insertion reaction takes place for x = 2 Li uptake. The corresponding refined values of the cell parameters are reported in Table 1.

During the first discharge, the intensities of the $CoSn_2$ peaks begin to decrease. The calculated ratio between the intensities of *121* Bragg peak obtained for the samples E and D ($I^E_{121}/I^D_{121} = 0.8$) shows that the intensity of this *121* line in the X-ray pattern obtained for x = 6.7 (sample E) is lower than that obtained for x = 5.7 (sample F). The dashed line area clearly represented on the XRD patterns of the C−E samples (Figure 2) points out the evolution of the initial *112* and *220* $CoSn_2$ lines with an increase in the intensity of the new broad peaks near 38.5−40.2° (2θ), which means the formation of a new phase. Identifying the new phase is difficult, because all Li−Sn compounds have strong diffraction peaks in this angle range.[20−22] Nevertheless, the extruded metallic cobalt, which is linked to Li−Sn formation, was not observed by X-ray measurements. This may be due to (i) the strongest Co peak, which occurs at about 44.2° (2θ),

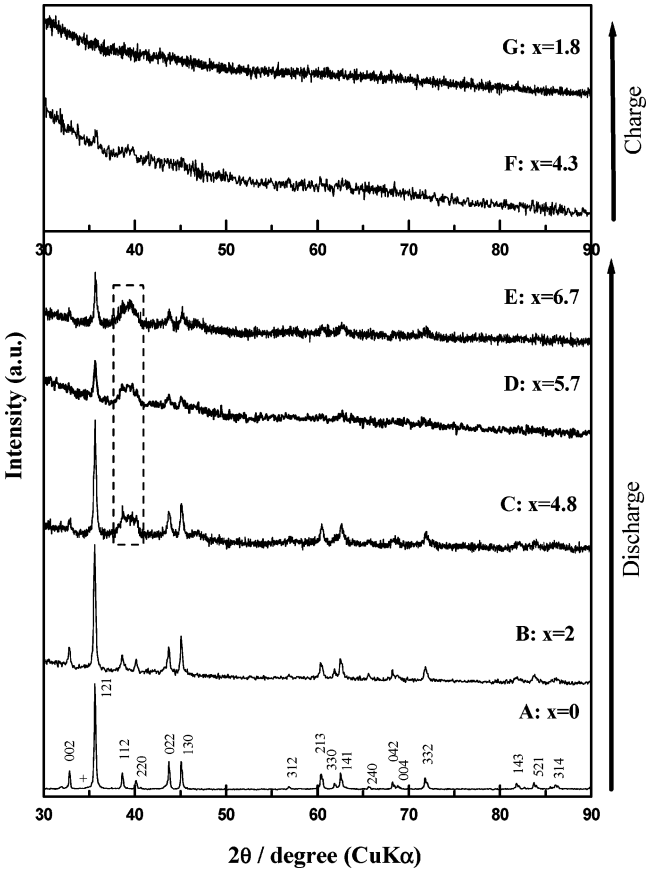

Figure 2. Powder X-ray diffraction patterns for $CoSn_2$ electrodes at various states of discharge to 0 V (samples A−E) and following charge to 1.5 V (samples F and G) at a rate of C/20. The dashed line points out the apparition (sample C) and the evolution (samples D and E) of the new broad peaks near 38.5−40.2° (2θ) during the discharge process.

being hidden by a $CoSn_2$ peak, or (ii) very small grains leading to broadened X-ray peaks. Previous works on ball-milled FeSn electrodes[23] suggested that the extruded inactive metal forms a thin layer, which prevents further Li reaction with the remaining intermetallic material, on the particle and/or grain surfaces. This may be the reason why the *121*, *022*, and *130* strongest lines of $CoSn_2$ are observed in the XRD diagram of the completely discharged sample E. The major changes occur during the succeeding charge. The reduction of the Li−Sn peak contribution was observed. Even if, for the F sample (0.55 V), we can still distinguish a very small contribution of the *121* peak of the $CoSn_2$, this is invisible on the end of the charge, sample G. The explication for the disappearance of $CoSn_2$ peaks is that during the charge process, the Li_xSn compound is transformed and some Li−Sn interactions and the Co-inactive film around $CoSn_2$ are destroyed to form the new amorphous phase. This affects the crystallinity of the $CoSn_2$ that is amorphized progressively during the oxidation process.

In situ ^{119}Sn Mössbauer Spectroscopy. Figure 3 shows the evolution of the whole spectra recorded during the discharge/charge cycle. All the spectra have been accurately analyzed to obtain the hyperfine parameters, i.e., isomer shift (δ), quadrupole splitting (Δ), total absorption, and contribution of each component.

(19) Le Caër, G.; Malaman, B.; Venturini, G.; Fruchart, D.; Roques, B. *J. Phys. F: Met. Phys.* **1985**, *15*, 1813.
(20) Dunlap, R. A.; Small, D. A.; MacNeil, D. D.; Obrovac, M. N.; Dahn, J. R. *J. Alloys Compd.* **1999**, *289*, 135.
(21) Chouvin, J.; Olivier-Fourcade, J.; Jumas, J.-C.; Simon, B.; Godivean, O. *Chem. Phys. Lett.* **1999**, *308*, 413.
(22) Robert, F.; Lippens, P. E.; Olivier-Fourcade, J.; Jumas, J. C ; Gillot, F.; Morcette, M.; Tarascon, J. M. *J. Solid State Chem.* **2006**, in press.
(23) Mao, O.; Dahn, J. R. *J. Electrochem. Soc.* **1999**, *146* (2), 414−422.

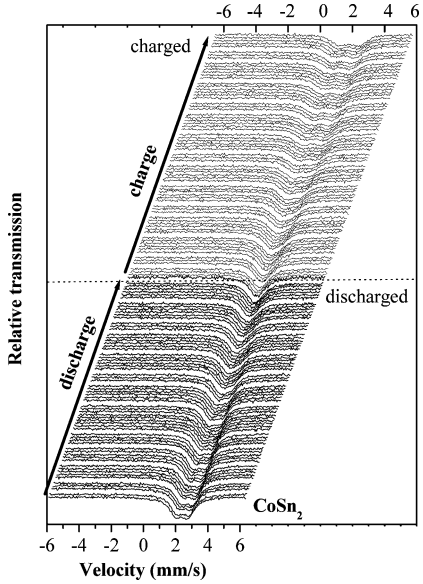

Figure 3. ^{119}Sn Mössbauer spectra recorded in situ during the first discharge process at a rate of C/20.

The plastic cell used for the in situ ^{119}Sn Mössbauer measurements allowed the reaction of 7.3 lithium ions, which corresponds to a total discharge capacity of about 660 A h kg^{-1}, and the removal of approximately 6 lithium ions during the following charge process, which means a total reversible capacity of 545 A h kg^{-1}. Figure 4a shows the voltage of the Li/$CoSn_2$ plastic cell vs reacted lithium ratio during the first discharge and charge process.

Figure 5 shows the most representative Mössbauer spectra obtained during discharge (see Figure 4a). The Mössbauer parameters are reported in Table 2. For $x = 0$ Li, the spectrum is that of $CoSn_2$. It was fitted with a doublet, as expected for the 8*h* Sn sites in the tetragonal structure. The hyperfine parameters, i.e., isomer shift ($\delta = 2.14(5)$ mm s^{-1}), quadrupole splitting ($\Delta = 0.77(9)$ mm s^{-1}) and line width ($\Gamma = 0.96(2)$ mm s^{-1}) were determined without ambiguity. The quadrupole splitting value is in line with the previous reported value by Le Caër et al. ($\Delta = 0.78 \pm 0.03$ mm s^{-1}).[19,24]

Up to $x \approx 0.5$ Li, the Mössbauer spectra were fitted with one doublet. The Mössbauer parameters do not change significantly and correspond to those of $CoSn_2$ (panels c and d of Figure 4).

For $0.5 \leq x \leq 7.3$ Li, the spectra were fitted with two components, i.e., a doublet assigned to $CoSn_2$ and a single Lorentzian peak at about 1.88 mm s^{-1}. The Mössbauer parameters of the $CoSn_2$ component, except line width and relative intensity, have been fixed, as these should not change throughout the cycling of the cell. The line widths of the two components were constrained to have the same value. The dashed lines on Figure 4 point out the positions of the isomer shift and the quadrupole splitting of $CoSn_2$. As illustrated in Figure 5, the intensity of the doublet from $CoSn_2$ (dot line) decreases and that of the other component increases. The isomer shift of the single line (∼1.88 mm s^{-1}) is lower than that of metallic β-Sn (2.56 mm s^{-1}) and

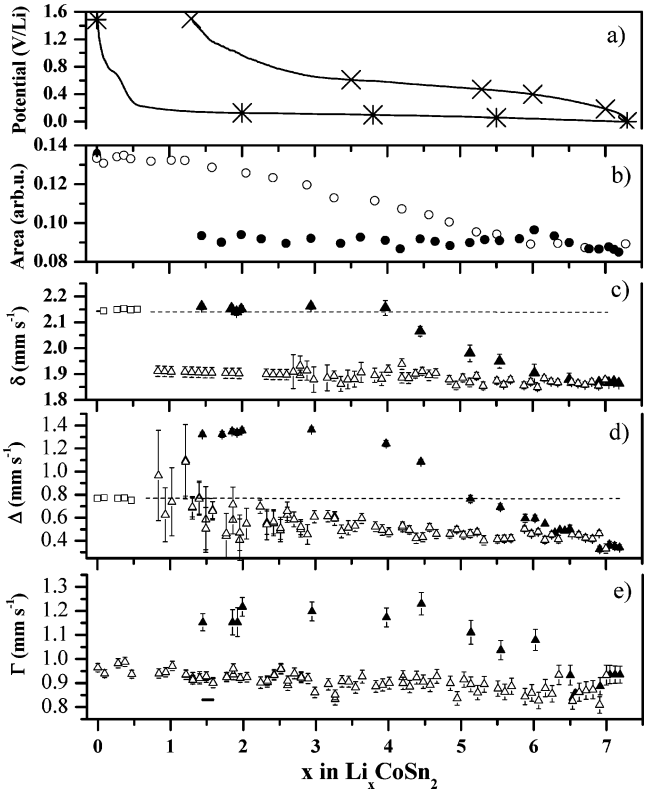

Figure 4. Evolution of the in situ Mössbauer parameters during electrochemical discharge and charge: (a) charge and discharge curve of the $CoSn_2$ electrode for the in situ plastic cell at rate of C/20; the symbols denote the compositions considered for the most representative Mössbauer spectra; (b) integrated spectrum area; (c) isomer shift; (d) quadrupole splitting; (e) line width; empty and filled symbols indicate the parameters evolution during the discharge and charge process, respectively. The dash lines in panels c and d point out the position of the constant values used for the $CoSn_2$ Mössbauer parameters.

is a feature of Li-rich Li_ySn compounds ($y = 3.5-4.4$).[20,22] The variations in the quadrupole splitting show a small decrease, between about 0.7 and 0.4 mm s^{-1}, during discharge with large dispersion in the higher values (Figure 4e).

The isomer shift of the Li_ySn component does not vary noticeably during discharge. This clearly indicates that y is constant and that no different Li−Sn compounds are formed during discharge. In order to obtain more information on this alloy, we have considered the following two-phase reaction

$$CoSn_2 + 2y\text{Li} \rightarrow 2\text{Li}_y\text{Sn} + \text{Co}\ (y = 3.5 \text{ or } 4.4) \quad (1)$$

The two values of y correspond to the two stable phases of the lithium-rich crystalline compounds. The resonant total absorption A decreases progressively all along the discharge reaction (Figure 4b), characterizing the formation of the new Li_ySn compound with a recoil-free fraction f_2 lower than that of $CoSn_2$ (f_1). This means that the relative contributions of $CoSn_2$ and Li_ySn given by the relative areas A_1 and A_2 of the two Mössbauer subspectra do not directly reflect the relative contributions N_1 and N_2 of the two species. To evaluate N_1 and N_2, it is necessary to know the $k = f_2/f_1$ ratio, which can be evaluated from the linear variations of A in the $x = 0.5-6.5$ range. We have obtained $k = 1-0.124y$, which gives $k = 0.57$ and 0.46 when $y = 3.5$ and 4.4,

(24) Jaén, J.; Varsanyi, M. L.; Kovacs, E.; Czaklo-Nagy, I.; Buzas, A.; Vértes, A.; Kiss, L. *Electrochim. Acta* **1984**; *29*, 8, 1119.

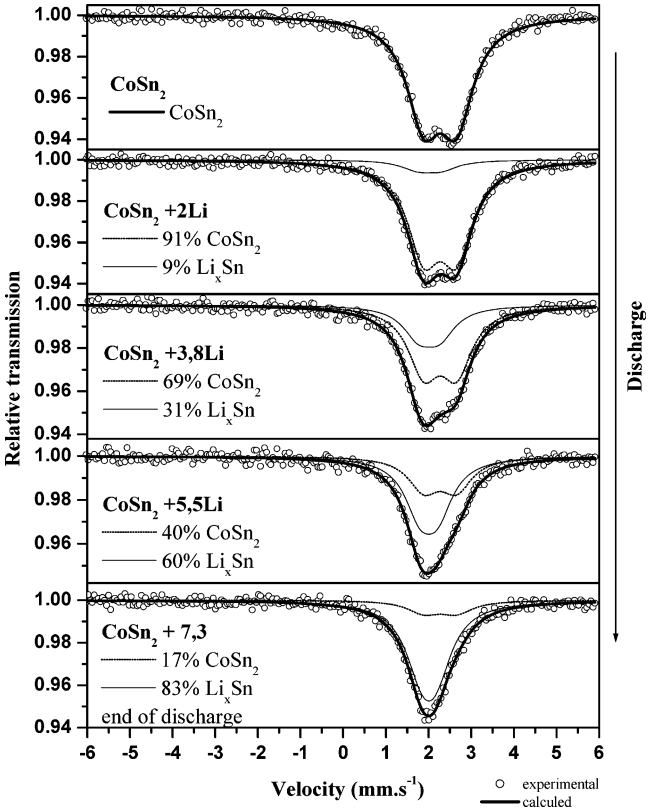

Figure 5. Most representative Mössbauer spectra recorded during the first discharge process at a rate of C/20.

Table 2. Hyperfine Parameters Obtained in the Refinement of the Most Representative in situ ^{119}Sn Mössbauer Spectra for the $CoSn_2$ Electrode in a Plastic Cell during the Discharge (isomer shift (δ), quadrupole splitting (Δ), line width at half-maximum (Γ), and Mössbauer relative contributions (C))

composition Li_xCoSn_2	δ (mm s^{-1})	Δ (mm s^{-1})	Γ (mm s^{-1})	C (%)	χ^2
$x = 0$ ($CoSn_2$)	2.14(5)	0.77(9)	0.96(2)	100	0.93
$x = 2$	2.14	0.77	0.92(2)	91	0.83
	1.89(3)	0.55(4)	0.92(2)	9	
$x = 3.8$	2.14	0.77	0.89(4)	69	0.99
	1.89(7)	0.52(3)	0.89(4)	31	
$x = 5.5$	2.14	0.77	0.88(2)	40	0.98
	1.88(3)	0.42(3)	0.88(2)	60	
$x = 7.3$	2.14	0.77	0.93(1)	17	0.85
	1.88(1)	0.33(4)	0.93(1)	83	

respectively. At the end of the discharge cycle ($x = 7.3$), the contribution of the Li_ySn component to the Mössbauer spectrum is $A_2 = 0.83$, which gives $N_2 = 0.89$ and 0.91 when $x = 7$ and 8.8, respectively. Thus, $CoSn_2$ was transformed into about 10% $CoSn_2$ and 90% Li_ySn. Such a transformation requires 6.3 Li when $y = 3.5$ and 7.9 Li when $y = 4.4$. Figure 4 shows that about 0.5 Li does not react with $CoSn_2$ at the beginning of the first discharge and the Mössbauer parameters of Li_ySn do not vary significantly in the $x = 6.5-7.3$ range. This suggests that the maximum number of Li reacting with $CoSn_2$ should be about 6−6.5. Thus, the composition of the Li_ySn should be close to that of Li_7Sn_2. The relative contributions N_1 and N_2 evaluated for $k = 0.57$ are shown in Figure 6.

The most representative ^{119}Sn Mössbauer spectra collected during the first charge are illustrated in Figure 7 (see Figure 4a), and the Mössbauer parameters are given in Table 3. For simplicity, all the spectra of the charge were fitted with two doublets corresponding to the remaining $CoSn_2$ and to the

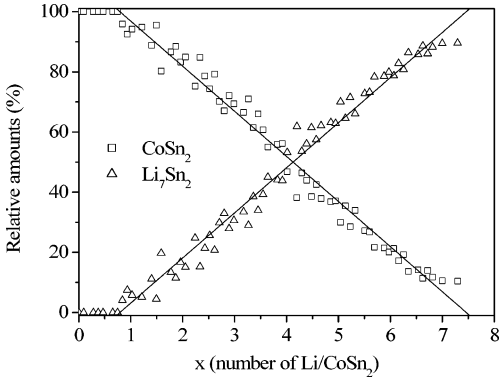

Figure 6. Relative contributions of $CoSn_2$ and Li_xSn ($x \approx 3.5$) components during the discharge process at a rate of C/20.

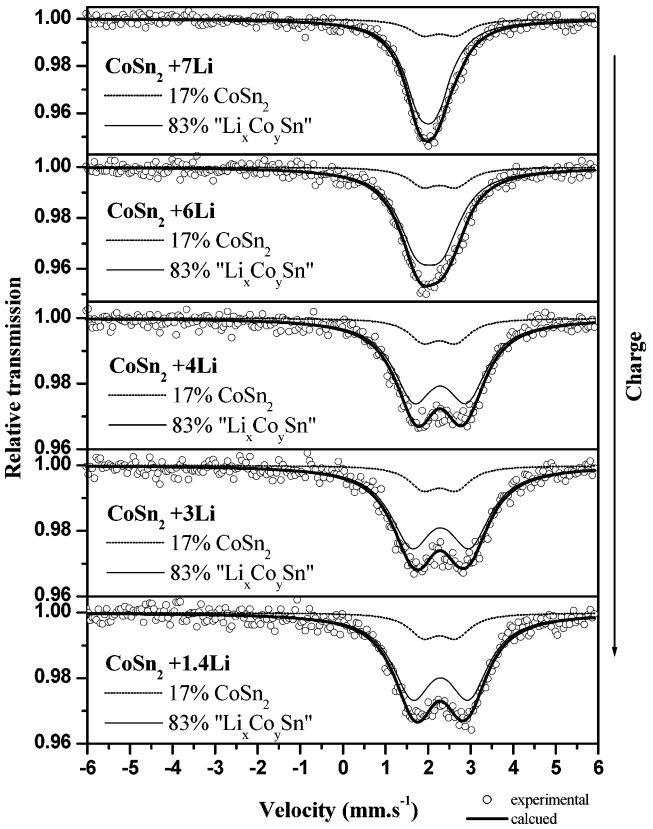

Figure 7. Most representative Mössbauer spectra recorded during the first charge process at a rate of C/20.

Table 3. Hyperfine Parameters Obtained in the Refinement of the Most Representative in situ ^{119}Sn Mössbauer Spectra for the $CoSn_2$ Electrode in a Plastic Cell during the Charge (isomer shift (δ), quadrupole splitting (Δ), line width at half-maximum (Γ), and Mössbauer relative contributions (C))

composition Li_xCoSn_2	δ (mm s^{-1})	Δ (mm s^{-1})	Γ (mm s^{-1})	C (%)	χ^2
$x = 7$	2.14	0.77	0.83	17	0.87
	1.87(1)	0.42(3)	0.89(4)	83	
$x = 6$	2.14	0.77	0.83	17	1.08
	1.90(3)	0.60(3)	1.08(4)	83	
$x = 4$	2.14	0.77	0.83	17	0.98
	2.16(8)	1.24(2)	1.17(4)	83	
$x = 3$	2.14	0.77	0.83	17	1.08
	2.16(3)	1.36(2)	1.19(4)	83	
$x = 1.4$	2.14	0.77	0.83	17	1.10
	2.16(2)	1.32(2)	1.15(4)	83	

transformation of the Li_ySn, respectively. The Mössbauer parameters and contribution of the $CoSn_2$ component were kept constant during the whole charge process. Figure 4c−e

shows the evolution of the Mössbauer parameters of the second component (filled symbols), which indicates continuous changes in the composition. The isomer shift value is increasing from 1.88 to 2.16 mm s^{-1} when the recharge process ends, which indicates both a decrease in the Li concentration in this phase and the back reaction of Sn from the modified Li−Sn compound with the Co atoms located at the grain boundaries. The attained value (2.16 mm s^{-1}) is close to the value of δ obtained for the raw $CoSn_2$ electrode material. The above-mentioned component ($\delta = 2.16(2)$ mm s^{-1}, $\Delta = 1.32(2)$ mm s^{-1}, $\Gamma = 1.15(4)$ mm s^{-1}) is referred to as Li_yCo_zSn compound with a composition close to that of $CoSn_2$. The y value in Li_yCo_zSn is very small. The other two parameters (Δ, Γ) are higher. This could be due to the effect of the surface Sn atoms (nanoparticles) or to amorphization. The formation of Sn that is expected to be produced by the delithiation of the Li−Sn compound was not observed during the charge process.

Proposed Mechanism. The correlation between the XRD results and in situ ^{119}Sn Mössbauer spectra interpretation allows us to put forward the following mechanism for the first discharge/charge cycle of the $CoSn_2$ electrode. The discharge curve of the plastic cell includes two stages. The first one is the introduction of Li into the $CoSn_2$ electrode between 2.5 and 0.2 V, leading to both SEI formation and a possible solid-solution insertion reaction, with or without very weak structure perturbation. The second stage is the transformation of $CoSn_2$, which leads to the formation, by a substitution/extraction reaction, of a "Li_7Sn_2"-type nanocompound and Co nanoparticles at the end of the discharge process at 0 V. The total reaction mechanism can be described by

$$CoSn_2 + 2yLi^+ + 2ye^- \rightarrow 2Li_ySn + Co\ (y \approx 3.5\ Li) \quad (2)$$

The reaction indicated by eq 2 is not complete, and the relative contribution of the unreacted $CoSn_2$ at the end of the first discharge was evaluated to be 10%.

On charge, the extraction of Li from the Li_7Sn_2 compound makes them react to Co nanoparticles. This leads to the formation of a new Li_yCo_zSn amorphous phase characterized by a strong Sn content and in which Li−Sn interactions still occur. This slightly lithiated phase, which was observed at the end of the charge process, is not observed in the X-ray diffraction patterns, which is due to the fact that nanosized and/or amorphous grains are formed.

Conclusion

This work has focused on (i) the analysis of the mechanisms that occur during the discharge/charge reactions of Li with $CoSn_2$; (ii) various studies of the structural changes induced by the introduction/extraction of lithium; and (iii) the microstructure of the resulting products.

The X-ray diffraction results give an incomplete picture of the processes that occur in the $CoSn_2$ electrode. Additional in situ ^{119}Sn Mössbauer measurements allow for a better understanding of the reactions that occur. Various two-step reactions were observed for the $CoSn_2$ electrode: an insertion solid solution is first obtained, followed by a substitution/extraction reaction that directly forms lithium-rich Li_xSn compounds ($x \approx 3.5$) and Co nanoparticles. This reaction was found to be incomplete; the relative contribution of unreacted $CoSn_2$ was estimated to be 10%. During the charge process, the transformation of this alloy into a new phase was observed and included back reaction with Co nanoparticles. This amorphous compound was referred to as Li_yCo_z-Sn, whose composition is close to that of the $CoSn_2$ phase. This compound is the active species for the next cycles of the cell.

Acknowledgment. This work was supported by ADEME, France, the Agence Nationale de la Recherche, France ("LIBAN" project), and ALISTORE Network of Excellence (Contract SES6-CT-2003-503532). The authors are grateful to Mathieu Morcrette from LCRS, Amiens, France, for the plastic cells fabrication.

CM062132I